Spatial Dependence of the Phonon-Limited Mobility in Arbitrarily Oriented Si-Nanowires

I.M. Tienda-Luna*, F.G. Ruiz, A. Godoy, E. González-Marín, and F. Gámiz
Dpto. Electrónica, Fac. Ciencias, Universidad de Granada. Av. Fuentenueva S/N, 18071 - Granada, Spain
* Email: isabelt@ugr.es

INTRODUCTION

The study of the transport properties of Si-Nanowires (NWs) is a research field of high interest [1], [2]. The spatial dependence of the low-field mobility and, in particular, the role of the corners is still not clear. Only recently, Lee et al. [3] have considered their impact on the mobility through the development of a Spatial Dependent Mobility (SDM) expression. In this work, we extend their approach to study the phonon-limited mobility (μ_{ph}) of arbitrarily oriented square NWs.

RESULTS

NWs with SiO_2 as gate insulator (T_{ins}=1nm), midgap metal gate, undoped body and width $W_{Si} \geq$ 5nm are considered. For these sizes, the effective mass (EM) approach provides accurate enough results [4], [5]. Two approaches for the SDM are used in this work. The first of them is proposed in [3] as:

$$SDM(x,y) = \frac{\sum_i |\Psi_i(x,y)|^2 \mu_i n_i}{\sum_i |\Psi_i(x,y)|^2 n_i} \quad (1)$$

where Ψ_i, μ_i and n_i are the i_{th} subband wave function, mobility and population, respectively. The alternative expression is defined as follows:

$$SDM2(x,y) = A \times \frac{\sum_i |\Psi_i(x,y)|^2 \mu_i n_i}{\sum_i n_i} \quad (2)$$

which combines the information provided by the SDM with the actual population of each subband (n_i). Fig. 1 shows the results for the SDM for NWs with $W_{Si} =$ 10nm. Three orientations are considered: (100)/[001] (first row), (110)/[001] (second row) and (01$\bar{1}$)/[011] (third row). First column figures were calculated using (1), where only the (100)/[001] NW was studied. For (110)/[001] and (01$\bar{1}$)/[011] NWs, the SDM is strongly correlated to the directions where the Δ_4 and Δ_2 valleys (respectively) get their highest confinement EM and thus their largest population. A complementary vision of these results can be found when using (2) (second column). As can be seen the SDM2 is higher at the corners of the NWs due to their larger electron density (ED). This effect is more noticeable in (110)/[001] NWs due to: *(i)* the higher SDM of the corner regions (Fig. 1(c)) and *(ii)* the larger ED near the corners. Fig. 2 shows the results for NWs with $W_{Si} =$ 5nm, where more homogeneous mobilities are achieved for SDM, while SDM2 grows at the center of the NWs. For both expressions, the largest values are attained by the (110)/[001] NW. Fig. 3 compares the contribution to the SDM2 of the first two subbands of the [100] valley for (110)/[001] and (100)/[001] NWs. As can be seen, the contribution of the first subband in the (110)/[001] device is higher, being the responsible for the total SDM2 increase near the center of the device. Fig. 4a shows $\mu_i \times n_i$ of each subband, which measures its relative contribution to the total mobility. For a wide range of charge density per unit length (N_i) values, only the first subband of Δ_4 valleys significantly contribute to the mobility in (110)/[001] NWs while also the second subbands are relevant in (100)/[001] devices (which is consistent with the result shown in Fig. 3. Fig. 4b compares the acoustic-phonon momentum relaxation time (τ_i^{ac}) for these two subbands at $V_G = 0.8$V (optical phonons are not considered to simplify the analysis [3]). As shown in the inset (where the rest of the components in the Kubo-Greenwood formula are depicted), only energy values below 0.15eV effectively contribute to the mobility. Thus, the smaller mobility achieved by the first subband of (100)/[001] NW is due to the reduction in τ_1^{ac} in this range of energies, caused by its higher proximity to the second subband. Since the mobility of the first subband governs the behavior of these small devices, (110)/[001] NWs achieve the highest μ_{ph} for $W_{Si} =$ 5nm NWs (Fig. 4c). For larger devices the analysis is more complex, as more subbands contribute to the mobility. However, the subband energy separation of Δ_4 valleys (not shown) is smaller for the (110)/[001] NW [6], reducing the mobility of the first subbands and thus lowering μ_{ph} (Fig. 4c).

ACKNOWLEDGMENT

Work supported by the projects P09-TIC-4873, FIS-2008-05805 and FIS-2011-26005). E. González-Marín also acknowledges the FPU program.

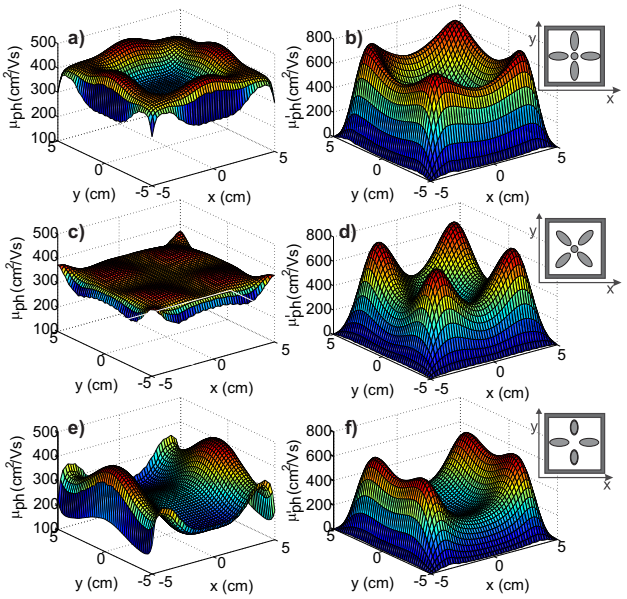

Fig. 1. SDM (left column) and SDM' (right column) of square NWs with $W_{Si} = 10$nm. (a) and (b): (100)/[001] NWs, (c) and (d): (110)/[001] NWs and (e) and (f): $(01\bar{1})$/[011] NWs (see insets).

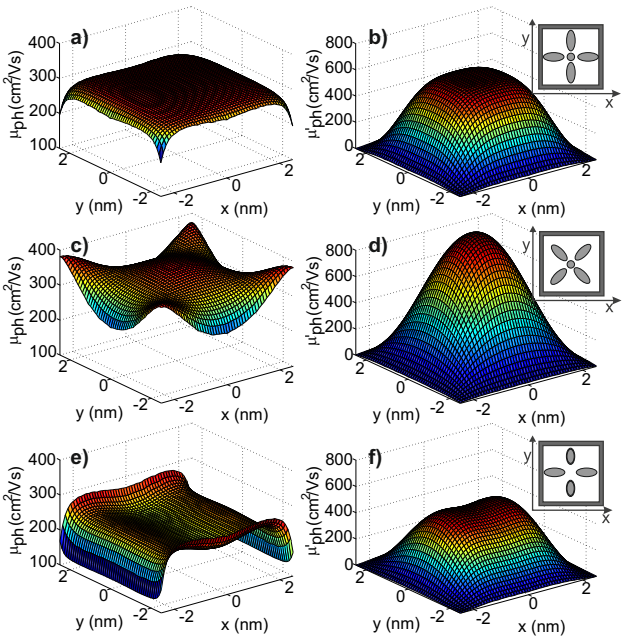

Fig. 2. SDM and SDM' of square NWs with $W_{Si} = 5$nm (same distribution as Fig. 1).

REFERENCES

[1] E. Ramayya et al., IEEE Trans. Nanotech., **6**, 1 (2007).
[2] S. Jin et al., J. App. Phys., **102**, 5 (2007).
[3] Y. Lee et al., J. App. Phys., **109**, 11 (2011).
[4] M. Bescond et al., Nanotech., **18**, (2007).
[5] J. Wang et al., IEEE Trans. Elec. Dev., **52**, 7 (2005).
[6] I.M. Tienda-Luna et al., EUROSOI 2011.

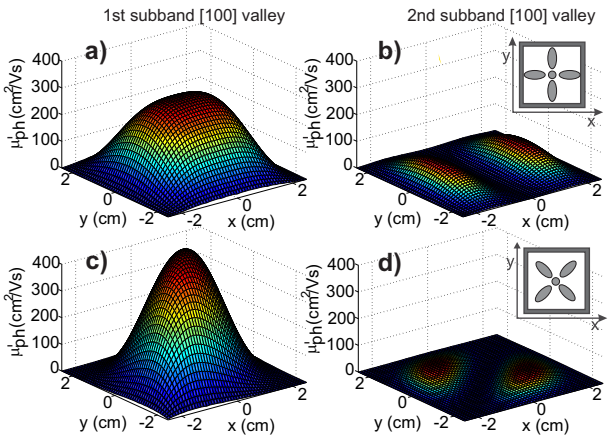

Fig. 3. Contribution to the SDM' of the first two subbands of Δ_4 valleys for (a) and (b): (100)/[001] NWs and (c) and (d): (110)/[001] NWs.

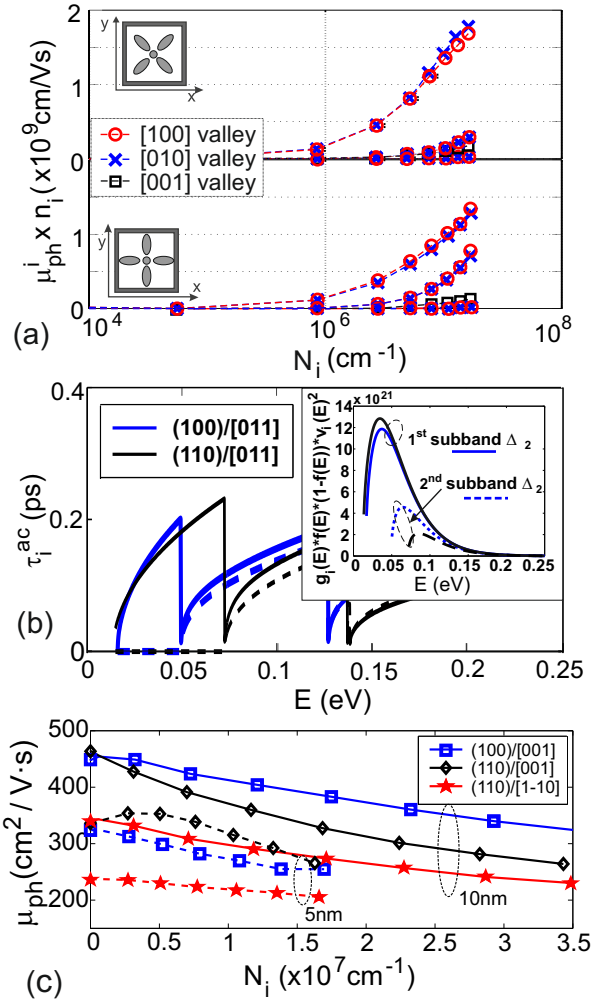

Fig. 4. Comparison between (100)/[001] and (110)/[001] NWs: (a) Contribution of i subband to the total mobility ($\mu^i_{ph} \times n_i$) vs. N_i, (b) τ_i vs. E and (in the inset) the rest of the parameters involved in Kubo-Greenwood formula vs. E, and (c)μ_{ph} vs. N_i for different orientations (solid-lines for $W_{Si} = 10$nm and dashed-lines for $W_{Si} = 5$nm).